Supporting Information

Yi and Schnitzer 10.1073/pnas.0901324106

SI Text

Tumor Cell Culture, Harvesting, and Immunoblot. B16 melanoma and LLC cell lines were grown in continuous culture for no more than 3 consecutive passages. Actively growing cells were trypsinized (0.25% trypsin/1 mM Na-EDTA; Gibco/BRL), resuspended in DMEM, counted, and injected s.c. into KO and WT mice. Western analysis was performed as described (1), using the following antibodies: AnxA1 rabbit polyclonal (Zymed); β-actin mouse monoclonal (Sigma); CD31 rat monoclonal (BD PharMingen); TIMP2, Nrp1 (neuropilin), and SphK1 rabbit polyclonal and Col18a1 rat monoclonal (Santa Cruz Biotechnology); CTGF, CXCL10, and Angpt2 rabbit polyclonal and MMP2 and FIGF mouse monoclonal (Abcam); and AKT1 rabbit polyclonal (Cell Signaling Technology).

Tumor Models. Tumor growth was monitored by measuring the longest (L) and shortest (W) diameters and the depth (H) of the gross tumor area. We also visually monitored the ulcerated area inside the gross tumor area at regular time intervals for 2 to 3 months. Tumor and necrotic volumes (V) were calculated as $V = 1/6\ (\pi LWH)$.

Histology and Immunofluorescent Staining. Paraffin-fixed and frozen blocks of tumor tissues from KO and WT mice were prepared, sectioned, and stained as described (2). For immunofluorescent staining, the frozen sections were fixed in 4% paraformaldehyde, followed by 3 washes in PBS solution, 30 min incubation in 3% BSA for blocking, 1 h incubation with primary antibody, 3 washes in PBS solution, 1 h incubation with fluorescently labeled secondary antibody, 3 washes in PBS solution, then mounting with Vectorshield mounting media containing DAPI.

Wound Healing Assay. The KO and WT mice were anesthetized by i.p. injection of ketamine/xylene. The mouse back was shaved and cleaned with 70% alcohol, and wounds were made as described (3). All wounds were left uncovered, some were sutured as stated in *Results* in the main text, and the mice were housed in individual cages postoperatively to keep them from scratching each other. The wounds were measured regularly and photographed.

Aortic Ring Assay. The rings of aorta from the KO and WT mice were obtained and cultured in matrigel by following the method of Nicosia et al. (4) with modifications. Aortas were collected from the mice and washed in DMEM, followed by sectioning into rings approximately 1 mm long and embedding into Matrigel in tissue culture wells. The aortic ring cultures were maintained for 1 week in MCDB131 (Gibco/BRL) supplemented with 2.5% mouse serum, 1% glutamine, 100 U/mL penicillin, and 100 μg/mL streptomycin, at 37 °C, 5% CO_2, followed by photography and counting of outgrown microvessels. For rescue experiments, adenovirus expressing WT mouse AnxA1 and adenovirus empty vector were prepared with AdEasy adenoviral vector system following the manufacturer's instructions (Stratagene). Adenoviral-infected aortic rings from KO mice were cultured on Matrigel in the same culture conditions described earlier.

1. Schnitzer JE, McIntosh DP, Dvorak AM, Liu J, Oh P (1995) Separation of caveolae from associated microdomains of GPI-anchored proteins. *Science* 269:1435–1439.
2. Oh P, et al. (2004) Subtractive proteomic mapping of the endothelial surface in lung and solid tumours for tissue-specific therapy. *Nature* 429:629–635.
3. Ashcroft GS, Horan MA, Ferguson MW (1997) The effects of ageing on wound healing: immunolocalisation of growth factors and their receptors in a murine incisional model. *J Anat* 190:351–365.
4. Nicosia RF, Zhu WH, Fogel E, Howson KM, Aplin AC (2005) A new ex vivo model to study venous angiogenesis and arterio-venous anastomosis formation. *J Vasc Res* 42:111–119.

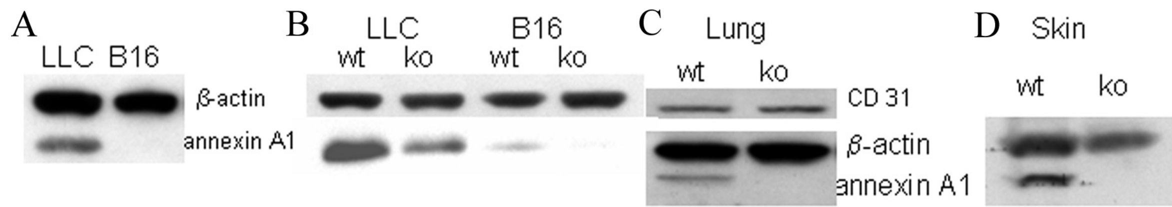

Fig. S1. AnxA1 expression in cell lines, tumor models, and host tissues. Different levels of AnxA1 expression were detected in (*A*) lysates of cultured tumor cells, (*B*) tumor lysates from LLC- and B16-derived tumors taken from KO and WT mice, and (*C* and *D*) normal host tissues from KO and WT mice. β-actin was used as a gel-loading control.

Fig. S2. AnxA1 plays a significant role in angiogenesis-related biological processes such as wound healing. Affymetrix mouse genome expression microarray analysis was performed on the B16 tumors s.c. grown in KO and WT mice. Systems analysis on the gene expression differences between KO and WT mice was performed using Genomatix software and the GO database. Z-scores for the biological processes are shown in a summary histogram of sequential mining of GO hierarchy for biological processes showing only statistically significant over-representation for ''response to stimulus'' culminating in ''wound healing.''

Fig. S3. Angiogenesis-related genes express differently in KO mice. The gene expression analysis was performed on the B16 tumors (*Tumor*) and aortas (*Aorta*) from KO and WT mice. (*A*) Expression profiles of 113 genes with expression level from low (black) to high (red) and 3 repeats (WT1, WT2, WT3, and KO1, KO2, KO3). (*B*) Differential expression of genes in angiogenesis pathways.

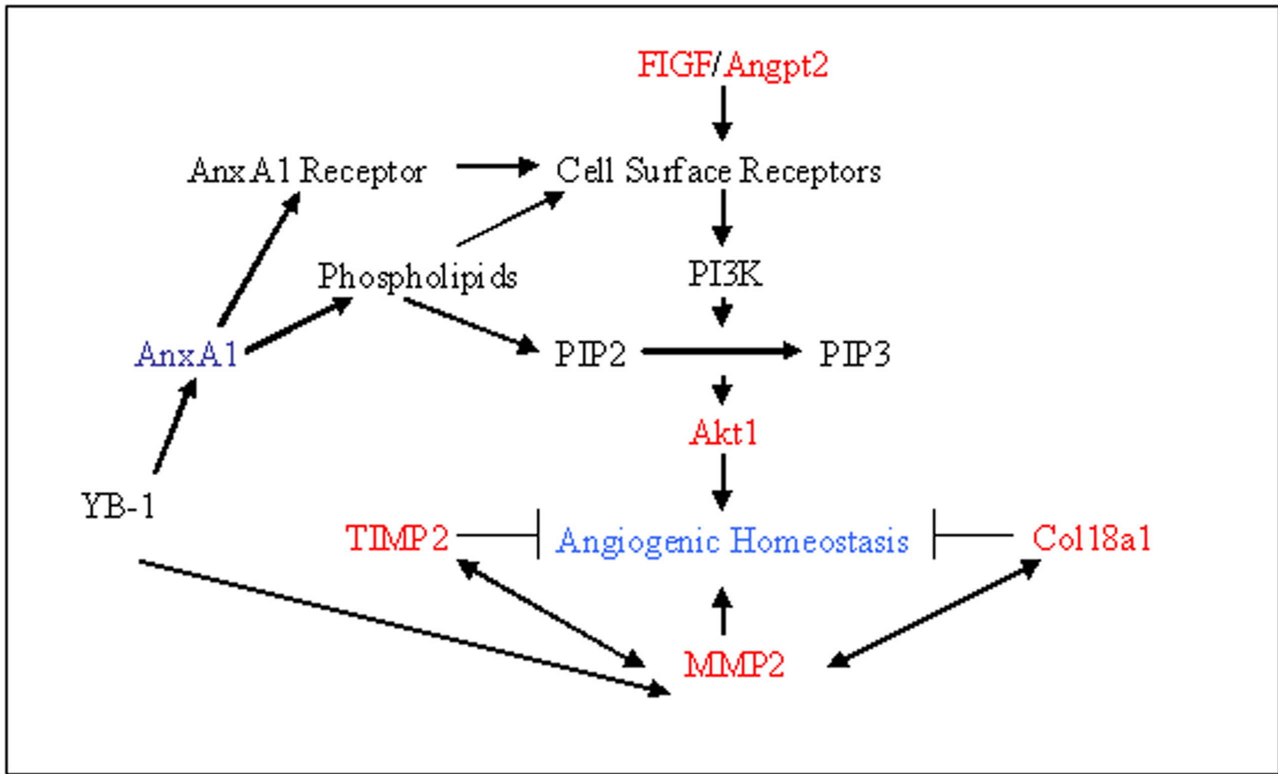

Fig. S4. A reset angiogenic switch. AnxA1 is a pro-angiogenic regulator in homeostasis of angiogenic state.

Table S1. Annexin A1 knockout and expression of angiogenesis-related genes

Pathway	Genes
Not Affected by Annexin A1 KO	
VEGF	VEGFα, VEGFβ, MAPK14
FGF	FGF1, FGF2, FGFR3
PDGF	PDGFα, PDGFβ
Eph	Efna1, Efna2, Efna3, Efnab2, Ephb4
Wnt	Fzd5
Ang-1	Angpt1
Delta	Notch4
Affected by Annexin A1 KO	
	TIMP2
	MMP2
	FIGF
	ECGF1
	Akt1
	Angpt2
	Col18a1